

MLP Memory: Language Modeling with Retriever-pretrained External Memory

Rubin Wei^{1*}, Jiaqi Cao^{1*}, Jiarui Wang¹, Jushi Kai¹, Qipeng Guo²

Bowen Zhou^{2,3}, Zhouhan Lin^{1,2†}

¹LUMIA Lab, Shanghai Jiao Tong University

²Shanghai Artificial Intelligence Laboratory

³Electronic Engineering, Tsinghua University

weirubinn@gmail.com, [†]lin.zhouhan@gmail.com

Abstract

While modern decoder-only LLMs achieve superior performance across various domains, hallucinations have risen to be a common problem in their generated text, hindering their application in knowledge-intensive tasks. Retriever-augmented generation (RAG) offers a solution, but the non-parametric nature of the retriever hinders its deep interaction with LLM. In this work, we propose to decouple memorization from the LLM decoder using a pretrained, differentiable external memory. The external memory is an MLP pretrained by imitating the behavior of a retriever on the entire pretraining dataset. Our resulting architecture, which comprises a transformer decoder and an external MLP memory pretrained on language modeling and retriever imitation respectively, demonstrates strong perplexity and performance on downstream tasks. Experiments show our architecture exhibits steeper power-law scaling with model size, achieving 17.5% and 24.1% improvement on WikiText-103 and Web datasets compared to decoder-only models while benefiting from added training without overfitting. We demonstrate superior performance on three hallucination benchmarks and nine memory-intensive tasks. Additionally, our approach delivers $80\times$ speedup over k NN-LM (500M tokens) and $1.3\times$ faster inference than decoder-only models. Unlike k NN-LM, which impairs reasoning, our MLP memory improves StrategyQA performance. We will open-source our code and models in the future.

1 Introduction

Decoder-only architectures such as GPT [1], LLaMA [17], Qwen [46], and DeepSeek [33] have achieved remarkable success in various tasks, including open-ended text generation [40], code completion [4], image synthesis [3], and multimodal reasoning [35]. However, it is widely recognized that the current decoder-only LLMs lack a reliable memory, suffering from hallucinations [61, 37]. The generated content could be fluent but factually incorrect or inconsistent.

To mitigate hallucinations, two different approaches have been widely adopted. First, alignment techniques such as supervised fine-tuning (SFT) have been widely applied, albeit incurring an alignment tax [32]. In most cases, it leads to degraded general capabilities or overly conservative outputs. On the other hand, by incorporating an external retriever, RAG [29, 43, 10, 23] is another effective approach to mitigate hallucination and enhance domain knowledge. However, the retriever’s reliance on query-key relevance estimation restricts its ability to handle complex interactions between memorized content and prevents efficient memory compression. Furthermore, the non-parametric retrieval process prevents gradient flow to the retriever during training, isolating it from the language model and hindering end-to-end optimization.

*Equal contribution.

[†]Zhouhan Lin is the corresponding author.

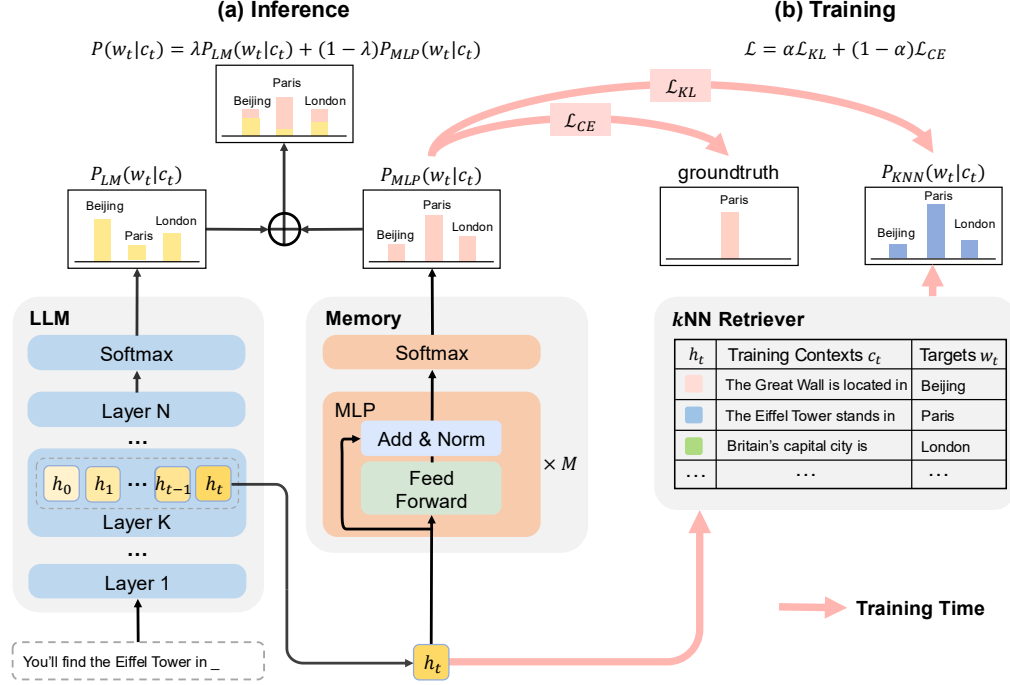


Figure 1: Overview of our overall architecture’s inference and training pipelines. (a) Inference: MLP memory processes context representations from a specific LLM layer, generating token probabilities that are interpolated with LLM outputs for final predictions. (b) Training: MLP memory is pretrained by imitating retriever behavior across the pretraining dataset. Representations from a specific LLM layer serve as both MLP memory inputs and kNN search queries to generate kNN distributions. Training employs a combination of Kullback-Leibler divergence [52] and cross-entropy loss [60].

In contrast to the decoder-only LLM architecture, neuroscience research in the past few decades has unveiled a clearly lateralized human brain[13, 44, 55, 11]. For most people, language processing is dominated by the left hemisphere[12], while memory formation is more related to the hippocampus[9]. This insight has inspired the development of memory-augmented models in machine learning. Early attempts to incorporate external memory were primarily task-specific. Memory Network [54] enabled read and write operations on a long-term memory. Similarly, Sparse Access Memory presents an end-to-end differentiable memory access scheme. However, these approaches were designed for specific downstream tasks and learned through task-specific loss functions, thereby restricting their general applicability. In the era of LLMs, research has increasingly focused on memory tokens to extend context length. Approaches such as Memory Transformers [2] incorporate trainable memory tokens to retain global context, while AutoCompressors [6] compress long contexts into summary vectors for efficient long-range modeling. Nevertheless, these memory tokens primarily function as working memory supplements, addressing context length limitations rather than serving as long-term memory capable of retaining information from the entire training corpus.

In this work, we propose an external memory for LLM that is pretrained to mimic a retriever on the entire pretraining dataset. Specifically, following the RAG setting in k NN-LM [27], this memory learns to map the LLM hidden state at a certain step to a vocabulary distribution matching the output of the k NN retriever. During inference, the LLM’s native output is interpolated with the retriever-pretrained output from the external memory. Our resulting architecture, illustrated in Figure 5, consists of a transformer decoder and an external MLP memory, each pretrained separately with different pretraining tasks. For our pretrained external memory, we aim to achieve the following features simultaneously:

- 1) **End-to-end differentiable.** Unlike the non-parametric nature of retrievers, our MLP memory is fully parameterized and allows gradient flow during training. This enables end-to-end joint optimization of the entire model architecture.

- 2) **Highly compressible memory.** The MLP memory compresses large datastores (e.g., 220GB for 100M tokens in k NN-LM) into a compact parametric form (e.g., 2.8GB for 700M parameters), facilitating efficient deployment without performance degradation.
- 3) **Low inference-time latency.** MLP memory eliminates costly retrieval operations, achieving $80\times$ faster inference than k NN-LM with a 500M-token datastore, and $1.3\times$ speedup over the decoder-only models. Notably, this performance advantage increases with context length.
- 4) **Scalable, general knowledge memorization, covering the whole training set.** MLP memory is trained on the entire pretraining dataset, not limited to the context level. It supports general knowledge retention and demonstrates stronger scaling behavior than decoder-only models.
- 5) **Long-term memory.** While existing memory tokens serve primarily as working memory by storing local context for immediate use, our MLP memory functions as a long-term repository of generalizable knowledge acquired during the pretraining phase.

Experimental results show that our new *decoder with external memory* architecture delivers significant advantages across multiple dimensions. Our architecture exhibits steeper power-law scaling with model size, achieving 17.5% and 24.1% improvement on WikiText-103 and Web datasets compared to decoder-only architectures, while continuing to benefit from additional training without overfitting. On downstream tasks, our architecture consistently outperforms both baseline models and k NN-LM approaches, reducing hallucinations across TruthfulQA, FACTOR, and HaluEval-Sum benchmarks while delivering performance gains across nine diverse memory-intensive tasks. We also achieve substantial inference efficiency with $80\times$ speedup over k NN-LM (500M tokens) and $1.3\times$ faster inference than decoder-only models, with efficiency advantages that increase with context length. Notably, while prior work has demonstrated that k NN-LM degrades reasoning abilities [14], our MLP memory actually enhances reasoning capabilities, improving StrategyQA [15] performance across all base models. These results underscore the distinctive potential of our parametric memory approach.

2 Related Work

Retrieval-Augmented Generation. RAG [29, 43, 10] offers a promising approach to mitigate hallucinations in language models by grounding generated text in external knowledge sources. Traditional RAG systems combine a retrieval component with a generative model, allowing LLMs to access information beyond their parametric knowledge. Despite improving factual accuracy, RAG systems face several limitations. Retrieval introduces significant latency, and coarse granularity often leads to fetching entire documents for specific facts. Moreover, the non-parametric retriever limits seamless integration with the LLM, as noted in recent studies [57]. Recent work, such as [50], explores enhanced retrieval and its interplay with the LLM’s internal priors. Our approach diverges by proposing a parametric memory that mimics non-parametric retrieval, eliminating explicit document retrieval while preserving knowledge augmentation benefits.

Memory-Augmented Language Models. Memory augmentation for language models has been explored through various architectures. Early work, such as Memory Network [54], introduced explicit read-write memory components, while later models like Memory Transformers [2] leveraged extended attention for in-context memorization. LongMem [53] further advanced the field by introducing a decoupled architecture, using the original frozen backbone LLM as a memory encoder to store long-term history. Similarly, MemoRAG [45] employed a dual-system design, using a lightweight, long-range module to build global memory for improved retrieval. While these approaches show promise, they primarily focus on extending context length for long-context modeling. In contrast, our MLP memory expands memory augmentation across the entire pre-training corpus rather than just the immediate context window. This allows for long-term memory of generalizable knowledge acquired during pre-training, distinguishing our method from conventional context-extension techniques.

MLP Architectures. Recent works have explored all-MLP architectures as alternatives to attention-based models. gMLP [34] showed that all-MLP models with Spatial Gating Units can match transformers in language modeling. Building on this, [56] proposed sparsely activated MLPs with mixture-of-experts (MoEs) that increase model capacity while maintaining computational efficiency, demonstrating superior training efficiency over transformer models. The role of MLP layers in transformer-based LLMs has attracted growing research interest, with studies [16] identifying that Feed-Forward Network (FFN) layers function as key-value memories, suggesting MLPs have a specialized role in knowledge memorization within LLMs. Despite these advances, few studies

have explored using all-MLP architectures to memorize embedding datastores for retrieval. Inspired by [16], which frames MLP layers as key-value stores, we propose pretraining an all-MLP memory that functions as a non-parametric retriever. We leverage the memorization capabilities of MLPs to create a compact, differentiable knowledge store that enhances LLM reliability.

3 Method

3.1 Preliminary: k -nearest neighbors language model

The k -nearest neighbors language model (k NN-LM) [27] augments a pre-trained neural language model (LM) by interpolating its parametric output distribution with a non-parametric distribution estimated via nearest neighbor retrieval from an external datastore. Specifically, given a context sequence of tokens $c_t = (w_1, \dots, w_{t-1})$, the next-token probability $p(w_t | c_t)$ is computed as:

$$p(w_t | c_t) = \lambda p_{kNN}(w_t | c_t) + (1 - \lambda) p_{LM}(w_t | c_t), \quad (1)$$

where $\lambda \in [0, 1]$ is the interpolation hyperparameter, p_{LM} denotes the original LM’s predicted distribution, and p_{kNN} is a retrieval-based distribution derived from an external datastore.

Datastore. The external datastore is constructed through a single forward pass over a text corpus. Let $f(\cdot)$ be the function that encodes a context sequence of tokens c_t into a fixed-dimensional vector using hidden representations from a pre-trained LM. For each training example (c_t, w_t) from our training set \mathcal{D} , we define a key-value pair (k_t, v_t) , where the key $k_t = f(c_t)$ is the vector representation of the context c_t , and the value v_t is the corresponding next token w_t . The full datastore $(\mathcal{K}, \mathcal{V})$ is then given by:

$$(\mathcal{K}, \mathcal{V}) = \{(f(c_t), w_t) \mid (c_t, w_t) \in \mathcal{D}\}. \quad (2)$$

Inference. At inference time, the pre-trained LM encodes the current context c into a query vector $f(c)$ and produces a parametric next-token distribution $p_{LM}(y | c)$. The query $f(c)$ is used to retrieve the k -nearest neighbors $\mathcal{N} = \{(k_i, v_i)\}_{i=1}^k$ from the datastore $(\mathcal{K}, \mathcal{V})$, based on a distance metric $d(\cdot, \cdot)$ (typically squared L^2 [27]). A non-parametric distribution p_{kNN} is then computed by applying a softmax over the negative distances of the retrieved keys, accumulating probability mass for tokens that appear in \mathcal{N} , while assigning zero probability to those not retrieved:

$$p_{kNN}(y | c) \propto \sum_{(k_i, v_i) \in \mathcal{N}} \mathbb{I}_{y=v_i} \exp(-d(k_i, f(c))). \quad (3)$$

k NN-LM enhances language modeling by integrating explicit memory for improved prediction, but its scalability is limited by considerable storage requirements and high-latency neighbor retrieval.

3.2 MLP Memory

3.2.1 Architecture

Our model architecture employs a novel decoupled framework, featuring a transformer decoder module for language generation and a memory module that collaborates with the decoder to provide contextual knowledge during generation. As the decoder module adheres to a standard decoder-only architecture, we omit further details here.

In designing the memory module, we observe that the retriever imitation task processes a single-vector representation without requiring token-mixing operations. Recent studies [16] have identified that FFN layers function as key-value memories, suggesting that MLPs play a specialized role in knowledge memorization within LLMs. Based on these insights, we propose pretraining an all-MLP memory that effectively functions as a non-parametric retriever.

3.2.2 Training Pipeline

The complete training pipeline for our overall model architecture comprises two phases: (i) standard language modeling for the transformer decoder, and (ii) retrieval imitation training for the MLP memory. Since the language modeling phase follows established LM training procedures, we focus our discussion primarily on the retrieval imitation training pipeline, as illustrated in Figure 5.

Step 1: Datastore Construction We construct the datastore $(\mathcal{K}, \mathcal{V})$ following the same way as vanilla k NN-LM, as detailed in Section 3.1. Notably, the training set serves as the text corpus, while the decoder module functions as a pre-trained LM.

Step 2: Pre-computed k NN Search For each training context (c_t, w_t) , we perform a k NN search using the query representation $f(c_t)$ over the datastore $(\mathcal{K}, \mathcal{V})$ constructed in Step 1. Since both the queries and the datastore originate from the same training set, the nearest neighbor corresponds to the ground-truth target. To prevent the supervision signal from collapsing into a near one-hot distribution, we exclude the ground truth target from the retrieved results. The remaining top- $(k-1)$ results $\mathcal{N}'\{(k_i, v_i)\}_{i=1}^{k-1}$ are then used to construct the k NN distribution y_i as shown in equation 3.

Step 3: Memory Module Training The above steps are performed offline and only once, resulting in a training dataset $(f(c_t), y_i)$ for the memory module. Unlike vanilla k NN-LM, which uses the input to the final FFN as the query, our experiments demonstrate that later-layer representations yield better performance for the memory module. Figure 5 illustrates the complete training pipeline.

Our experiments in Section 4.4 demonstrate that relying solely on cross-entropy (CE) loss [60] leads to rapid overfitting of the memory module, as it tends to memorize specific token patterns without generalizing effectively. By incorporating Kullback-Leibler (KL) divergence [52] loss, we achieve significantly better results by leveraging the rich probabilistic information encoded in the k NN distribution. The KL term encourages the memory module’s predictions p_{MLP} to align with the information-rich k NN distribution y_i , which we formally defined as:

$$\mathcal{L}_{KL} = \sum_{w \in \mathcal{V}} y_i(w) \log \frac{y_i(w)}{p_{MLP}(w)}, \quad (4)$$

where $y_i(w)$ is the probability of token w in the k NN distribution, and $p_{MLP}(w)$ represents the memory module’s output probability for token w given context embedding $f(c_t)$.

Complementing this, the CE loss ensures that the model’s predictions remain accurate with respect to the ground-truth labels and is defined as:

$$\mathcal{L}_{CE} = - \sum_{w \in \mathcal{V}} \mathbb{1}_{w=w_t} \log p_{MLP}(w), \quad (5)$$

where $\mathbb{1}$ is the indicator function and w_t represents the next token of the context c_t .

The final training objective for the memory module is formulated as a weighted sum of these two losses:

$$\mathcal{L} = \alpha \cdot \mathcal{L}_{KL} + (1 - \alpha) \cdot \mathcal{L}_{CE}, \quad (6)$$

where $\alpha \in [0, 1]$ is a tunable hyperparameter.

3.3 Inference Efficiency Analysis

Table 1 presents the computational cost breakdown for both Transformer and MLP architectures in terms of FLOPs per token. As demonstrated, the primary difference in computational efficiency stems from the absence of attention mechanisms in pure MLP models.

By comparing these computational requirements, we derive the theoretical speed ratio between the Transformer (denoted as $FLOPs_t$) and the MLP models (denoted as $FLOPs_m$):

$$\frac{FLOPs_t}{FLOPs_m} \approx \frac{4n_{layer}d_{model}(2d_{attn} + d_{ff}) + 2n_{layer}n_{ctx}d_{attn}}{6n_{layer}d_{model}d_{ff}} = 1 + \frac{n_{ctx}}{12d_{model}}, \quad (7)$$

with the standard $d_{attn} = d_{ff}/4 = d_{model}$.

This relationship in Equation 7 reveals that MLPs maintain a consistent computational advantage across all context lengths, with the efficiency gap widening as context length increases.

4 Experiments

In Sec.4.1, we analyze the scaling behavior of models augmented with MLP memory through power-law fitting. Next, in Sec. 4.2 and Sec.4.3, we evaluate its capability in reducing hallucinations and improving performance on memory-intensive tasks, respectively. Finally, Sec. 4.4 presents ablation studies and analyses designed to understand the effectiveness of the MLP memory module.

Table 1: Flops per Token at inference time. Following [26], we analyze computational requirements for Transformer and MLP architectures where n_{layer} (number of layers), d_{model} (dimension of the residual stream), d_{ff} (dimension of the intermediate feed-forward layer), d_{attn} (dimension of the attention output), n_{heads} (number of attention heads per layer), n_{ctx} (the length of input context), n_{vocab} (vocabulary size). $C_{forward}$ denotes computational cost per token inference step.

Operation	FLOPs per Token(Transformer)	FLOPs per Token(MLP)
Embed	$4d_{model}$	—
Attention: QKV	$2n_{layer}d_{model}3d_{attn}$	—
Attention: Mask	$2n_{layer}n_{ctx}d_{attn}$	—
Attention: Project	$2n_{layer}d_{attn}d_{model}$	—
Feedforward	$2n_{layer}2d_{model}d_{ff}$	$3n_{layer}2d_{model}d_{ff}$
De-embed	$2d_{model}n_{vocab}$	$2d_{model}n_{vocab}$
Total(Non-Embedding)	$C_{forward} = 4n_{layer}d_{model}(2d_{attn} + d_{ff}) + 2n_{layer}n_{ctx}d_{attn}$	$C_{forward} = 6n_{layer}d_{model}d_{ff}$

4.1 Scaling law

Setup. We conduct scaling law experiments using standard decoder-only models and our overall model architecture. As baselines, we use four GPT-2 [47] variants with increasing parameter counts: GPT2-small (124M), GPT2-medium (345M), GPT2-large (774M), and GPT2-xl (1.5B). For MLP memory, we define three configurations: small (124M), medium (335M), and large (774M) that align with the scaling trend of standard architectures. The MLP memory module is externally integrated with a matching-sized GPT-2 variant, resulting in total parameter counts of approximately 248M, 710M, and 1.5B for the small, medium, and large configurations, respectively. All models are trained on two datasets: WikiText-103 [38] (around 100M tokens) and a mixed Web dataset (around 600M tokens). Following [48], our Web dataset combines diverse knowledge sources relevant to common NLP tasks, including WikiText-103, Amazon Reviews [19], CC-NEWS [18], and IMDB [36].

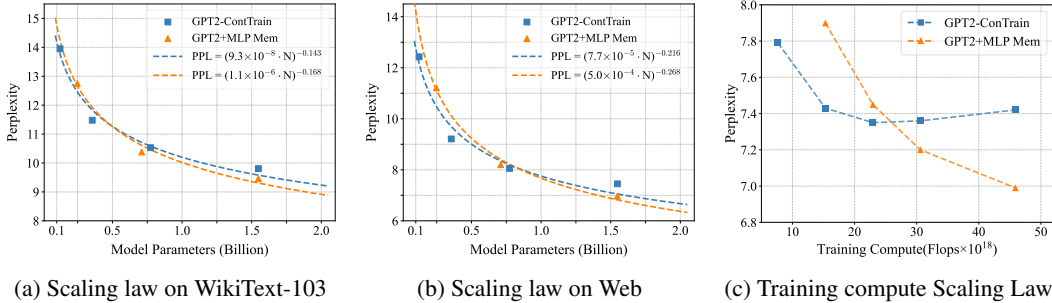


Figure 2: Power-law scaling behavior with model size N and training compute C . (a) Scaling results compare the continued training of GPT2 (GPT2-ConTrain) with our overall model architecture (GPT2+MLP Mem) under fixed compute. Our fitted curve shows a 17.5% exponent improvement on WikiText-103. (b) On the larger Web dataset, our architecture exhibits stronger scaling gains from increased data size, with an exponent improvement of 24.1%. (c) At the GPT2-xl scale, our architecture continues to benefit from additional training on the Web dataset without overfitting.

Scaling law with model parameters N . Following [26], we model perplexity scaling as $PPL = (\beta \cdot N)^\gamma$. Under fixed compute, we compare our architecture to continued GPT-2 training on WikiText-103 and Web datasets in terms of test perplexity scaling with model size N . Results in Figure 2 show our architecture demonstrates a steeper scaling curve than the decoder-only model, indicating improved scaling efficiency. The power-law scaling laws on WikiText-103 can be expressed as:

$$PPL_d = (9.3 \cdot 10^{-8} N)^{-0.143} \quad \text{and} \quad PPL_m = (1.1 \cdot 10^{-6} N)^{-0.168} \quad (8)$$

where PPL_d and PPL_m denote the test perplexity of the decoder model and our architecture, respectively. The corresponding power-law scaling laws on the Web dataset are as follows:

$$PPL_d = (7.7 \cdot 10^{-5} N)^{-0.216} \quad \text{and} \quad PPL_m = (5.0 \cdot 10^{-4} N)^{-0.268} \quad (9)$$

These results highlight the superior scaling efficiency of our overall model architecture compared to the standard decoder-only baseline, on both WikiText-103 and the Web dataset.

Scaling law with training compute C . We further examine how model performance scales with training compute C while keeping model size fixed. At the GPT2-xl scale, we conduct experiments on the Web dataset, measuring test perplexity after varying amounts of training flops. As illustrated in Figure 2 (c), our overall model architecture achieves significantly lower perplexity with increasing training compute, with no signs of overfitting. This suggests that the retriever imitation pretraining task is more challenging and continues to benefit from additional compute.

4.2 Hallucination Reduction with MLP Memory

In addition to perplexity improvements, we evaluate the effectiveness of our architecture in reducing hallucination on three benchmark datasets: TruthfulQA [31], FACTOR [39], and HaluEval-Sum [30]. Using Llama-2-7B [51], Llama-3-8B [17], and Mistral-7B-v0.3 [24] as base models, we build retrieval datastores from our Web dataset following the implementation in [14]. We train a corresponding MLP memory module for each model (1.2B parameters for Llama-2-7B, 1.6B for Llama-3-8B, and 1.5B for Mistral-7B-v0.3) and interpolate its output probabilities with the base model at inference time. All metrics are reported with higher values indicating better performance.

Table 2: Truthfulness scores (%) on three benchmarks under the setup of [25]. We compare decoder-only models, CPT models trained by continued pretraining on the Web dataset, LoRA [20], RAG [22], the k NN-LM baseline, and our proposed MLP Memory (denoted as MLP Mem), trained to imitate k NN retrieval and combined with the base model via interpolation at inference. We conducted experiments with 5 random seeds and report means. Bold numbers indicate the best performance.

Models	TruthfulQA			FACTOR		HaluEval-Sum			AVG
	MC1	MC2	MC3	Expert	News	Precision	Acc-A	Acc-H	
Llama2-7B	26.58	41.88	18.94	63.56	71.72	48.66	49.28	38.56	44.90
+CPT	26.83	42.93	19.28	63.55	67.47	42.39	46.45	31.15	42.50
+LoRA	28.22	42.85	19.52	72.88	67.95	46.61	47.92	43.63	46.20
+RAG	27.46	42.30	18.89	69.06	70.55	40.66	44.63	34.49	43.51
+ k NN-LM	26.46	42.27	19.12	64.83	71.04	49.09	49.55	36.68	44.88
+MLP Mem	26.10	43.96	20.11	63.98	72.78	53.49	51.94	40.64	46.62
Llama3-8B	29.87	47.43	22.19	66.95	75.87	48.98	48.48	35.35	46.89
+CPT	30.50	48.60	23.98	68.64	62.93	47.17	45.30	20.82	43.49
+LoRA	29.24	47.80	22.18	71.61	66.40	48.72	47.91	38.91	46.60
+RAG	28.35	46.16	21.54	74.57	73.26	46.07	45.16	40.77	46.99
+ k NN-LM	29.11	47.48	22.30	68.88	74.51	48.63	47.96	35.07	46.74
+MLP Mem	29.35	48.50	23.10	67.80	76.06	49.43	49.16	36.91	47.54
Mistral-7B-v0.3	28.60	46.11	21.55	66.95	75.28	72.50	53.60	20.68	48.16
+CPT	23.16	40.49	18.46	58.47	67.08	45.00	43.70	39.77	42.01
+LoRA	28.86	45.56	21.50	68.64	73.06	40.75	47.55	19.14	43.13
+RAG	29.24	45.81	21.59	74.15	74.22	43.75	49.40	8.04	43.28
+ k NN-LM	29.11	46.53	21.82	66.10	75.80	77.48	53.35	16.97	48.40
+MLP Mem	28.58	46.69	21.87	66.53	75.28	73.46	53.80	21.17	48.42

Results in Table 2 show that MLP memory consistently outperforms base models and all baselines across three hallucination benchmarks. CPT suffers from catastrophic forgetting, showing degraded performance across all models. LoRA achieves mixed results with strong FACTOR Expert scores but inconsistent overall gains. RAG performs well on certain metrics but exhibits severe brittleness on HaluEval-Sum Acc-H (e.g., 8.04% for Mistral-7B). While k NN-LM shows competitive performance, it remains less stable than our approach. In contrast, MLP Memory achieves the highest average scores for all three base models (46.62%, 47.54%, 48.42%), with notable gains in TruthfulQA MC2/MC3 and HaluEval-Sum benchmarks. By training the memory module separately and combining it through interpolation at inference, we preserve original model capabilities while enhancing factual accuracy, providing a new perspective for addressing hallucination without compromising generative capabilities.

4.3 Improving Memory-Intensive Task Performance with MLP Memory

To further assess the capability of the MLP memory, we test on memory-intensive tasks from [14] across three categories: 1) sentiment classification, including SST-2 [49], movie review (MR) [41], customer review (CR) [21], Rotten Tomatoes (RT) [42], and a variant of hyperpartisan news detection (HYP) [28]; 2) textual entailment, which assesses the relationship between two sentences by determining whether one entails, contradicts, or is neutral with respect to the other, including CommitmentBank (CB) [8] and Recognizing Textual Entailment (RTE) [7]; 3) topic classification, aiming at identifying the main topic of a document. We use AG News (AGN) [58] and Yahoo [59]. We use the same inference models and retrieval datastores as in [14] and our hallucination experiments.

Table 3: Accuracy (%) comparison on various memory-intensive tasks. Vanilla model results (first row in each section) and k NN-LM results are taken directly from [14], while +MLP Mem refers to our MLP Memory module. We conducted experiments with 5 random seeds and report means. Bold numbers indicate the best performance.

Models	Sentiment Classification					Textual.		Topic.		AVG
	SST2	MR	CR	RT	HYP	CB	RTE	AGN	Yahoo	
Llama2-7B	84.02	83.10	74.55	79.74	64.15	50.00	66.06	81.30	59.37	71.37
+CPT	72.92	80.95	66.60	79.73	54.06	46.42	65.36	87.32	51.10	67.16
+LoRA	75.67	80.00	70.60	81.33	53.48	48.21	60.28	77.42	56.03	67.00
+RAG	84.02	82.05	84.75	80.20	48.83	46.42	53.42	80.26	57.53	68.61
+ k NN-LM [14]	84.68	82.85	76.95	79.46	64.15	51.79	66.43	81.46	58.83	71.84
+MLP Mem	85.67	82.50	83.25	79.27	64.16	51.79	65.34	83.51	59.47	72.77
Llama3-8B	86.54	83.80	79.10	79.46	59.30	64.29	70.76	79.17	58.87	73.48
+CPT	84.56	85.10	83.55	78.33	54.45	62.50	58.12	83.43	53.93	71.55
+LoRA	79.35	83.90	85.25	78.98	55.03	57.14	68.95	81.35	55.73	71.74
+RAG	89.07	84.55	74.15	83.95	49.22	62.50	60.64	82.86	59.03	71.77
+ k NN-LM [14]	87.04	83.50	80.45	79.55	59.30	71.43	61.37	79.33	58.93	73.43
+MLP Mem	86.00	83.55	78.15	80.02	58.91	67.86	71.48	79.64	58.90	73.83
Mistral-7B-v0.3	81.82	79.35	81.90	75.32	56.59	71.43	76.17	73.57	56.63	72.53
+CPT	87.25	82.95	82.50	77.48	60.07	57.14	52.71	83.11	51.56	70.53
+LoRA	86.54	83.20	75.15	80.11	59.49	57.14	69.67	65.46	57.12	70.43
+RAG	85.61	80.85	65.25	80.48	63.95	73.21	65.34	75.55	59.06	72.14
+ k NN-LM [14]	81.77	79.30	82.15	75.05	56.78	67.86	76.17	73.55	56.63	72.14
+MLP Mem	81.82	79.70	81.65	78.24	63.95	78.57	76.90	79.50	58.00	75.37

Table 3 shows MLP memory consistently outperforms both vanilla models, CPT, LoRA, RAG and k NN-LM across memory-intensive tasks, achieving the highest average accuracies with Llama-2-7B (72.77%), Llama-3-8B (73.83%), and Mistral-7B-v0.3 (75.37%).

Among baseline methods, CPT suffers from performance degradation, which aligns with recent findings by Cheng et al. [5] showing that continued pretraining drastically hurts prompting abilities. LoRA shows limited improvements, often underperforming vanilla models (e.g., 67.00% vs 71.37% for Llama-2-7B), while RAG exhibits unstable performance, particularly on textual entailment tasks. Although k NN-LM provides modest gains, our MLP memory module surpasses it across all model variants, with particularly strong performance on Mistral-7B-v0.3 (75.37% vs 72.14%). These results demonstrate that our MLP memory module effectively emulates retrieval capabilities in a fully parametric architecture, providing an efficient alternative to k NN-LM without sacrificing performance on tasks requiring strong memory capabilities.

4.4 Ablation Study and Analysis

Impact of Loss Weighting. We examine how balancing KL and CE losses affects retriever imitation performance by varying α from 0.0 to 1.0. As Figure 3(a) shows, extreme values produce suboptimal results—low values prevent the MLP memory from learning from the k NN distribution, while high values cause overfitting to the language modeling objective. The optimal balance occurs at $\alpha = 0.4$, indicating both objectives are necessary. KL divergence leverages the information-rich k NN

distribution, enabling more effective generalization, while CE loss provides essential token-level prediction accuracy. This balanced approach prevents overfitting while maintaining predictive power.

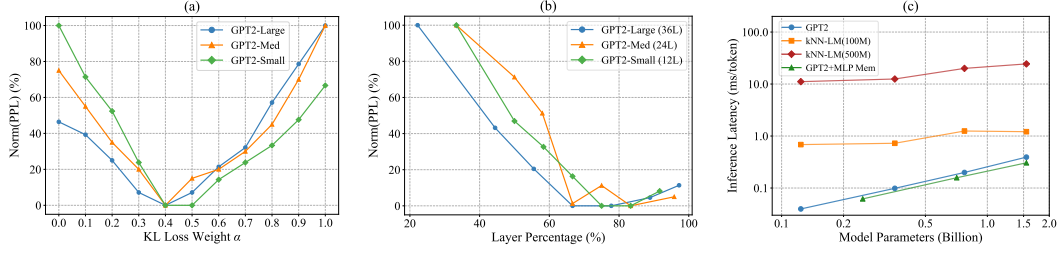


Figure 3: Ablation studies and efficiency analysis: (a) Impact of KL loss weight α on retriever imitation. Lower PPL (min-max normalized for clarity) indicates better performance, with optimal balance at $\alpha = 0.4$. (b) Impact of input layer depth on MLP memory performance across model sizes. Layer percentage denotes depth in the decoder stack (e.g., 70% corresponds to layer 25 in GPT2-large). (c) Inference latency comparison. Our MLP memory achieves $1.3\times$ speedup over the decoder baseline, and is $4\times/80\times$ faster than k NN-LM with 100M/500M-token datastores, respectively.

Which Layer Provides the Best Representation for MLP Memory? While k NN-LM performs best using the input to the final feedforward layer as the retrieval key, our MLP memory consistently achieves optimal performance at around 70% of network depth, regardless of model scale. Our finding aligns with Memorizing Transformers [2], which also selected around 75% depth for optimal retrieval performance. We evaluate GPT2-small (12 layers), GPT2-medium (24 layers), and GPT2-large (36 layers), attaching the MLP memory to various transformer blocks. As shown in Figure 3 (b), the x-axis indicates relative depth (20%–100%), and the y-axis shows min-max normalized perplexity (0% = best, 100% = worst). This consistent pattern across all model sizes contrasts with the k NN-LM convention of using final-layer representations.

Inference Latency Comparison. We compare the inference efficiency of three approaches: standard autoregressive decoders (GPT-2), retrieval-based k NN-LM, and our overall model architecture. Decoder models suffer from quadratic latency growth with sequence length due to attention mechanisms and key-value caching requirements. k NN-LM introduces significant computational overhead during generation through dynamic nearest-neighbor search over large external datastores, with costs scaling dramatically as retrieval databases grow. As Figure 3 (c) illustrates, our overall model architecture (GPT2+MLP Mem) achieves $1.3\times$ speedup over the decoder-only baseline, $4\times$ faster generation than k NN-LM with 100M tokens, and $80\times$ faster than k NN-LM with 500M tokens. These evaluations were conducted using a context length of 512, with efficiency gains becoming more pronounced at longer contexts as analyzed in Eq. 7, since MLP memory avoids the quadratic scaling of attention.

Impact on Reasoning Capabilities. We further evaluate our MLP memory on StrategyQA, a benchmark requiring multi-step reasoning and factual knowledge. As shown in Table 4, CPT shows inconsistent results with significant performance drops, particularly with Mistral-7B-v0.3, degrading accuracy by over 7% with COT prompting. k NN-LM also often hurts performance (e.g., -1.7% on Llama2-7B with COT). In contrast, MLP memory achieves consistent gains across all models, both with and without COT, with particularly strong improvements on Llama3-8B ($+1.62\%$ with COT). **Notably, while prior work has demonstrated that k NN-LM degrades reasoning abilities [14], our method enhances them.** This indicates that parametric retrieval captures richer information than non-parametric retrieval, benefiting both factual accuracy and reasoning.

Table 4: StrategyQA accuracy (%) with or without chain-of-thought (COT) prompting.

Models	w. COT	w/o. COT
Llama2-7B	60.69	52.40
+CPT	59.91	51.57
+ k NN-LM	58.99	51.31
+MLP Mem	61.14	52.58
Llama3-8B	64.23	55.28
+CPT	64.75	49.60
+ k NN-LM	63.62	57.42
+MLP Mem	65.85	55.46
Mistral-7B-v0.3	70.39	59.08
+CPT	62.57	54.49
+ k NN-LM	68.86	59.43
+MLP Mem	70.44	59.08

5 Conclusion

In this work, we presented a novel architecture that decouples memorization from the transformer decoder using a pretrained, differentiable external MLP memory that imitates retriever behavior. This overall model architecture is end-to-end differentiable. The MLP memory functions as a true long-term memory, pretrained on the entire training corpus. Additionally, the external memory is highly compressible (reducing storage from 220GB to 2.8GB for a 100M tokens datastore), and eliminates costly retrieval operations, achieving $80\times$ faster inference than k NN-LM(500M) and $1.3\times$ speedup over decoder-only models. Our architecture demonstrates stronger scaling behavior than decoder-only models, substantially reduces hallucinations, and improves performance on memory-intensive tasks. Surprisingly, contrary to prior work showing k NN-LM degrades reasoning abilities, our MLP memory enhances reasoning capabilities, improving StrategyQA performance across all base models. This confirms our neuroscience-inspired hypothesis that separating memorization from generation is a promising direction for advancing language models.

6 Limitation

Due to computational resource constraints, our current implementation trained the MLP memory on at most 600M tokens, with the Web dataset being our largest corpus, while future work will scale this to billions or even hundreds of billions of tokens to fully explore the potential performance benefits. Additionally, while we eliminate retrieval costs during inference, our approach requires a one-time preprocessing overhead to execute the three k NN-LM steps (datastore construction, index building, and k NN distribution generation) needed to produce training targets for the MLP memory.

References

- [1] Tom B. Brown, Benjamin Mann, Nick Ryder, Melanie Subbiah, Jared Kaplan, Prafulla Dhariwal, Arvind Neelakantan, Pranav Shyam, Girish Sastry, Amanda Askell, Sandhini Agarwal, Ariel Herbert-Voss, Gretchen Krueger, Tom Henighan, Rewon Child, Aditya Ramesh, Daniel M. Ziegler, Jeffrey Wu, Clemens Winter, Christopher Hesse, Mark Chen, Eric Sigler, Mateusz Litwin, Scott Gray, Benjamin Chess, Jack Clark, Christopher Berner, Sam McCandlish, Alec Radford, Ilya Sutskever, and Dario Amodei. Language models are few-shot learners, 2020.
- [2] Mikhail S. Burtsev, Yuri Kuratov, Anton Peganov, and Grigory V. Sapunov. Memory transformer, 2021.
- [3] Mark Chen, Alec Radford, Rewon Child, Jeff Wu, Heewoo Jun, David Luan, and Ilya Sutskever. Generative pretraining from pixels. In *Proceedings of the 37th International Conference on Machine Learning*, ICML’20. JMLR.org, 2020.
- [4] Mark Chen, Jerry Tworek, Heewoo Jun, Qiming Yuan, Henrique Ponde De Oliveira Pinto, Jared Kaplan, Harri Edwards, Yuri Burda, Nicholas Joseph, Greg Brockman, et al. Evaluating large language models trained on code. *arXiv preprint arXiv:2107.03374*, 2021.
- [5] Daixuan Cheng, Shaohan Huang, and Furu Wei. Adapting large language models to domains via reading comprehension. *arXiv preprint arXiv:2309.09530*, 2023.
- [6] Alexis Chevalier, Alexander Wettig, Anirudh Ajith, and Danqi Chen. Adapting language models to compress contexts, 2023.
- [7] Ido Dagan, Bill Dolan, Bernardo Magnini, and Dan Roth. Recognizing textual entailment: Rational, evaluation and approaches—erratum. *Natural Language Engineering*, 16(1):105–105, 2010.
- [8] Marie-Catherine De Marneffe, Mandy Simons, and Judith Tonhauser. The commitmentbank: Investigating projection in naturally occurring discourse. In *proceedings of Sinn und Bedeutung*, volume 23, pages 107–124, 2019.
- [9] Robert J Douglas. The hippocampus and behavior. *Psychological bulletin*, 67(6):416, 1967.

- [10] Luyu Gao, Xueguang Ma, Jimmy Lin, and Jamie Callan. Precise zero-shot dense retrieval without relevance labels, 2022.
- [11] Michael S Gazzaniga. Brain—corpus callosum: Review of the split brain. *Journal of Learning Disabilities*, 8(9):568–569, 1975.
- [12] Michael S Gazzaniga. *The ethical brain*. Dana press, 2005.
- [13] Michael S Gazzaniga. Forty-five years of split-brain research and still going strong. *Nature Reviews Neuroscience*, 6(8):653–659, 2005.
- [14] Shangyi Geng, Wenting Zhao, and Alexander M Rush. Great memory, shallow reasoning: Limits of k nn-lms. *arXiv preprint arXiv:2408.11815*, 2024.
- [15] Mor Geva, Daniel Khashabi, Elad Segal, Tushar Khot, Dan Roth, and Jonathan Berant. Did aristotle use a laptop? a question answering benchmark with implicit reasoning strategies. *Transactions of the Association for Computational Linguistics*, 9:346–361, 2021.
- [16] Mor Geva, Roei Schuster, Jonathan Berant, and Omer Levy. Transformer feed-forward layers are key-value memories. *arXiv preprint arXiv:2012.14913*, 2020.
- [17] Aaron Grattafiori, Abhimanyu Dubey, Abhinav Jauhri, Abhinav Pandey, Abhishek Kadian, Ahmad Al-Dahle, Aiesha Letman, Akhil Mathur, Alan Schelten, Alex Vaughan, et al. The llama 3 herd of models. *arXiv preprint arXiv:2407.21783*, 2024.
- [18] Felix Hamborg, Norman Meuschke, Corinna Breiteringer, and Bela Gipp. news-please: A generic news crawler and extractor, March 2017.
- [19] Ruining He and Julian McAuley. Ups and downs: Modeling the visual evolution of fashion trends with one-class collaborative filtering. In *proceedings of the 25th international conference on world wide web*, pages 507–517, 2016.
- [20] Edward J Hu, Yelong Shen, Phillip Wallis, Zeyuan Allen-Zhu, Yanzhi Li, Shean Wang, Lu Wang, Weizhu Chen, et al. Lora: Low-rank adaptation of large language models. *ICLR*, 1(2):3, 2022.
- [21] Mingqing Hu and Bing Liu. Mining and summarizing customer reviews. In *Proceedings of the Tenth ACM SIGKDD International Conference on Knowledge Discovery and Data Mining*, KDD ’04, page 168–177, New York, NY, USA, 2004. Association for Computing Machinery.
- [22] Gautier Izacard, Mathilde Caron, Lucas Hosseini, Sebastian Riedel, Piotr Bojanowski, Armand Joulin, and Edouard Grave. Unsupervised dense information retrieval with contrastive learning. *arXiv preprint arXiv:2112.09118*, 2021.
- [23] Gautier Izacard, Patrick Lewis, Maria Lomeli, Lucas Hosseini, Fabio Petroni, Timo Schick, Jane Dwivedi-Yu, Armand Joulin, Sebastian Riedel, and Edouard Grave. Atlas: Few-shot learning with retrieval augmented language models, 2022.
- [24] Albert Q. Jiang, Alexandre Sablayrolles, Arthur Mensch, Chris Bamford, Devendra Singh Chaplot, Diego de las Casas, Florian Bressand, Gianna Lengyel, Guillaume Lample, Lucile Saulnier, L  lio Renard Lavaud, Marie-Anne Lachaux, Pierre Stock, Teven Le Scao, Thibaut Lavril, Thomas Wang, Timoth  e Lacroix, and William El Sayed. Mistral 7b, 2023.
- [25] Jushi Kai, Tianhang Zhang, Hai Hu, and Zhouhan Lin. Sh2: Self-highlighted hesitation helps you decode more truthfully. *arXiv preprint arXiv:2401.05930*, 2024.
- [26] Jared Kaplan, Sam McCandlish, Tom Henighan, Tom B Brown, Benjamin Chess, Rewon Child, Scott Gray, Alec Radford, Jeffrey Wu, and Dario Amodei. Scaling laws for neural language models. *arXiv preprint arXiv:2001.08361*, 2020.
- [27] Urvashi Khandelwal, Omer Levy, Dan Jurafsky, Luke Zettlemoyer, and Mike Lewis. Generalization through memorization: Nearest neighbor language models, 2020.

- [28] Johannes Kiesel, Maria Mestre, Rishabh Shukla, Emmanuel Vincent, Payam Adineh, David Corney, Benno Stein, and Martin Potthast. SemEval-2019 task 4: Hyperpartisan news detection. In Jonathan May, Ekaterina Shutova, Aurelie Herbelot, Xiaodan Zhu, Marianna Apidianaki, and Saif M. Mohammad, editors, *Proceedings of the 13th International Workshop on Semantic Evaluation*, pages 829–839, Minneapolis, Minnesota, USA, June 2019. Association for Computational Linguistics.
- [29] Patrick Lewis, Ethan Perez, Aleksandra Piktus, Fabio Petroni, Vladimir Karpukhin, Naman Goyal, Heinrich Küttler, Mike Lewis, Wen tau Yih, Tim Rocktäschel, Sebastian Riedel, and Douwe Kiela. Retrieval-augmented generation for knowledge-intensive nlp tasks, 2021.
- [30] Junyi Li, Xiaoxue Cheng, Wayne Xin Zhao, Jian-Yun Nie, and Ji-Rong Wen. Halueval: A large-scale hallucination evaluation benchmark for large language models, 2023.
- [31] Stephanie Lin, Jacob Hilton, and Owain Evans. Truthfulqa: Measuring how models mimic human falsehoods, 2022.
- [32] Yong Lin, Hangyu Lin, Wei Xiong, Shizhe Diao, Jianmeng Liu, Jipeng Zhang, Rui Pan, Haoxiang Wang, Wenbin Hu, Hanning Zhang, Hanze Dong, Renjie Pi, Han Zhao, Nan Jiang, Heng Ji, Yuan Yao, and Tong Zhang. Mitigating the alignment tax of rlhf, 2024.
- [33] Aixiu Liu, Bei Feng, Bing Xue, Bingxuan Wang, Bochao Wu, Chengda Lu, Chenggang Zhao, Chengqi Deng, Chenyu Zhang, Chong Ruan, et al. Deepseek-v3 technical report. *arXiv preprint arXiv:2412.19437*, 2024.
- [34] Hanxiao Liu, Zihang Dai, David R. So, and Quoc V. Le. Pay attention to mlps, 2021.
- [35] Haotian Liu, Chunyuan Li, Qingyang Wu, and Yong Jae Lee. Visual instruction tuning. *Advances in neural information processing systems*, 36:34892–34916, 2023.
- [36] Andrew L. Maas, Raymond E. Daly, Peter T. Pham, Dan Huang, Andrew Y. Ng, and Christopher Potts. Learning word vectors for sentiment analysis. In Dekang Lin, Yuji Matsumoto, and Rada Mihalcea, editors, *Proceedings of the 49th Annual Meeting of the Association for Computational Linguistics: Human Language Technologies*, pages 142–150, Portland, Oregon, USA, June 2011. Association for Computational Linguistics.
- [37] Joshua Maynez, Shashi Narayan, Bernd Bohnet, and Ryan McDonald. On faithfulness and factuality in abstractive summarization, 2020.
- [38] Stephen Merity, Caiming Xiong, James Bradbury, and Richard Socher. Pointer sentinel mixture models, 2016.
- [39] Dor Muhlgay, Ori Ram, Inbal Magar, Yoav Levine, Nir Ratner, Yonatan Belinkov, Omri Abend, Kevin Leyton-Brown, Amnon Shashua, and Yoav Shoham. Generating benchmarks for factuality evaluation of language models, 2024.
- [40] OpenAI, Josh Achiam, Steven Adler, Sandhini Agarwal, Lama Ahmad, Ilge Akkaya, Florenzia Leoni Aleman, Diogo Almeida, Janko Altschmidt, Sam Altman, and Shyamal Anadkat. Gpt-4 technical report, 2024.
- [41] Bo Pang and Lillian Lee. Seeing stars: exploiting class relationships for sentiment categorization with respect to rating scales. In *Proceedings of the 43rd Annual Meeting on Association for Computational Linguistics*, ACL ’05, page 115–124, USA, 2005. Association for Computational Linguistics.
- [42] Bo Pang and Lillian Lee. Seeing stars: Exploiting class relationships for sentiment categorization with respect to rating scales. In *Proceedings of the ACL*, 2005.
- [43] Baolin Peng, Michel Galley, Pengcheng He, Hao Cheng, Yujia Xie, Yu Hu, Qiuyuan Huang, Lars Liden, Zhou Yu, Weizhu Chen, and Jianfeng Gao. Check your facts and try again: Improving large language models with external knowledge and automated feedback, 2023.
- [44] Yair Pinto, David A Neville, Marte Otten, Paul M Corballis, Victor AF Lamme, Edward H F de Haan, Nicoletta Foschi, and Mara Fabri. Split brain: divided perception but undivided consciousness. *Brain*, 140(5):1231–1237, 2017.

- [45] Hongjin Qian, Zheng Liu, Peitian Zhang, Kelong Mao, Defu Lian, Zhicheng Dou, and Tiejun Huang. Memorag: Boosting long context processing with global memory-enhanced retrieval augmentation. In *Proceedings of the ACM on Web Conference 2025*, pages 2366–2377, 2025.
- [46] Qwen, :, An Yang, Baosong Yang, Beichen Zhang, Binyuan Hui, Bo Zheng, Bowen Yu, Chengyuan Li, Dayiheng Liu, Fei Huang, Haoran Wei, Huan Lin, Jian Yang, Jianhong Tu, Jianwei Zhang, Jianxin Yang, Jiaxi Yang, Jingren Zhou, Junyang Lin, Kai Dang, Keming Lu, Keqin Bao, Kexin Yang, Le Yu, Mei Li, Mingfeng Xue, Pei Zhang, Qin Zhu, Rui Men, Runji Lin, Tianhao Li, Tianyi Tang, Tingyu Xia, Xingzhang Ren, Xuancheng Ren, Yang Fan, Yang Su, Yichang Zhang, Yu Wan, Yuqiong Liu, Zeyu Cui, Zhenru Zhang, and Zihan Qiu. Qwen2.5 technical report, 2025.
- [47] Alec Radford, Jeffrey Wu, Rewon Child, David Luan, Dario Amodei, Ilya Sutskever, et al. Language models are unsupervised multitask learners. *OpenAI blog*, 1(8):9, 2019.
- [48] Weijia Shi, Julian Michael, Suchin Gururangan, and Luke Zettlemoyer. Nearest neighbor zero-shot inference. In Yoav Goldberg, Zornitsa Kozareva, and Yue Zhang, editors, *Proceedings of the 2022 Conference on Empirical Methods in Natural Language Processing*, pages 3254–3265, Abu Dhabi, United Arab Emirates, December 2022. Association for Computational Linguistics.
- [49] Richard Socher, Alex Perelygin, Jean Wu, Jason Chuang, Christopher D. Manning, Andrew Ng, and Christopher Potts. Recursive deep models for semantic compositionality over a sentiment treebank. In David Yarowsky, Timothy Baldwin, Anna Korhonen, Karen Livescu, and Steven Bethard, editors, *Proceedings of the 2013 Conference on Empirical Methods in Natural Language Processing*, pages 1631–1642, Seattle, Washington, USA, October 2013. Association for Computational Linguistics.
- [50] Weihang Su, Yichen Tang, Qingyao Ai, Junxi Yan, Changyue Wang, Hongning Wang, Ziyi Ye, Yujia Zhou, and Yiqun Liu. Parametric retrieval augmented generation, 2025.
- [51] Hugo Touvron, Louis Martin, Kevin Stone, Peter Albert, Amjad Almahairi, Yasmine Babaei, Nikolay Bashlykov, Soumya Batra, Prajjwal Bhargava, Shruti Bhosale, et al. Llama 2: Open foundation and fine-tuned chat models. *arXiv preprint arXiv:2307.09288*, 2023.
- [52] Tim Van Erven and Peter Harremoos. Rényi divergence and kullback-leibler divergence. *IEEE Transactions on Information Theory*, 60(7):3797–3820, 2014.
- [53] Weizhi Wang, Li Dong, Hao Cheng, Xiaodong Liu, Xifeng Yan, Jianfeng Gao, and Furu Wei. Augmenting language models with long-term memory. *Advances in Neural Information Processing Systems*, 36:74530–74543, 2023.
- [54] Jason Weston, Sumit Chopra, and Antoine Bordes. Memory networks, 2015.
- [55] David Wolman. A tale of two halves. *Nature*, 483(7389):260–263, 2012.
- [56] Ping Yu, Mikel Artetxe, Myle Ott, Sam Shleifer, Hongyu Gong, Ves Stoyanov, and Xian Li. Efficient language modeling with sparse all-mlp, 2022.
- [57] Lingxi Zhang, Yue Yu, Kuan Wang, and Chao Zhang. Arl2: Aligning retrievers for black-box large language models via self-guided adaptive relevance labeling. *arXiv preprint arXiv:2402.13542*, 2024.
- [58] Xiang Zhang, Junbo Zhao, and Yann LeCun. Character-level convolutional networks for text classification. *Advances in neural information processing systems*, 28, 2015.
- [59] Xiang Zhang, Junbo Zhao, and Yann LeCun. Character-level convolutional networks for text classification. *Advances in neural information processing systems*, 28, 2015.
- [60] Zhilu Zhang and Mert Sabuncu. Generalized cross entropy loss for training deep neural networks with noisy labels. *Advances in neural information processing systems*, 31, 2018.
- [61] Chunting Zhou, Graham Neubig, Jiatao Gu, Mona Diab, Paco Guzman, Luke Zettlemoyer, and Marjan Ghazvininejad. Detecting hallucinated content in conditional neural sequence generation, 2021.

A Models

GPT-2. GPT-2 [47] is a unidirectional transformer-based language model developed by OpenAI and trained on the WebText [47] dataset. The model family consists of four variants with increasing parameter counts: GPT-2 Small (124M parameters), Medium (345M), Large (774M), and XL (1.5B). It adopts a decoder-only architecture with layer normalization and learned positional embeddings. Widely used as a benchmark in language modeling and transfer learning, GPT-2 has demonstrated the effectiveness of large-scale unsupervised pretraining. The official implementation and checkpoints are available at: <https://huggingface.co/openai-community/gpt2>.

Llama-2-7B. Llama-2-7B [51] is a decoder-only transformer model developed by Meta AI. It is part of the Llama 2 family, designed for efficient training and high performance on a wide range of natural language tasks. Trained on 2 trillion tokens of diverse public data, Llama 2-7B employs rotary positional embeddings (RoPE), SwiGLU activation functions, and grouped-query attention. It demonstrates strong performance in both zero-shot and few-shot settings, particularly in instruction-following tasks. The weights and documentation are available at: <https://huggingface.co/meta-llama/Llama-2-7b-hf>.

Llama-3-8B. Llama-3-8B [17] is an enhanced version of the Llama series, released by Meta AI in 2024. It incorporates improvements in training data scale, tokenizer design, and architecture efficiency. Specifically, Llama 3 uses a larger, more diverse training corpus, fine-grained tokenization, and architectural refinements such as improved attention scaling and better initialization schemes. Llama-3-8B achieves state-of-the-art performance among models of similar scale across multiple benchmarks. More details and model weights can be found at: <https://huggingface.co/meta-llama/Meta-Llama-3-8B>.

Mistral-7B-v0.3. Mistral-7B-v0.3 [24] is an open-weight, decoder-only transformer model developed by Mistral AI. This version builds upon the original Mistral-7B by refining training procedures and hyperparameters. It features grouped-query attention, sliding window attention, and uses a high-quality mix of public datasets for training. Mistral-7B is optimized for performance and inference efficiency, excelling in multilingual and code generation tasks. The model and release details are available at: <https://huggingface.co/mistralai/Mistral-7B-v0.3>.

B Datasets

WikiText-103. WikiText-103 [38] is a widely used benchmark for autoregressive language modeling derived from Wikipedia text. It consists of 103M training tokens, with 217K and 245K tokens in the validation and test sets, respectively, and has a 250K word-level vocabulary. The dataset is available at: <https://huggingface.co/datasets/Salesforce/wikitext>.

Web. The Web dataset is a heterogeneous corpus constructed by aggregating several publicly available sources that cover diverse domains relevant to common NLP tasks. According to the work [48, 14], it includes WikiText-103 [38], Amazon Reviews [19], CC-NEWS [18], and IMDB [36]. This mixture captures both formal and informal language, user-generated content, and a range of topics from news to product reviews. The dataset is available at: <https://huggingface.co/datasets/wentingzhao/knn-prompt-datastore>.

TruthfulQA. TruthfulQA [31] is a benchmark designed to evaluate the truthfulness of language models in open-ended question answering. It consists of 817 questions, each accompanied by multiple reference answers, and supports both generation and discrimination tracks. In the discrimination setting, each question includes sets of true and false reference answers. We compute the likelihood of each answer conditioned on the question and derive three multiple-choice metrics—MC1, MC2, and MC3—to assess the model’s ability to prefer truthful over false information. MC1 measures whether the model assigns the highest likelihood to the most accurate answer; MC2 sums the normalized probabilities over all correct answers; and MC3 evaluates whether the model assigns a higher average likelihood to true answers than to false ones. The dataset is available at: https://huggingface.co/datasets/truthfulqa/truthful_qa.

FACTOR. FACTOR [39] focuses on contextual consistency and evaluates how likely language models are to produce factual content. It formulates factuality as a text completion task, where models must distinguish the correct factual continuation from several nonfactual alternatives, given a shared prefix.

The benchmark comprises two subsets: Expert-FACTOR (236 examples) and News-FACTOR (1,036 examples). Factual accuracy is assessed based on whether the model assigns the highest probability to the correct completion. The dataset is available at: <https://github.com/AI21Labs/factor>.

HaluEval-Sum. HaluEval [30] is a benchmark for evaluating hallucination in language model outputs. We adopt its summarization track, which consists of 10,000 document-summary pairs, each labeled as either hallucinated or factual. For each instance, the model is asked to determine whether the summary contains factual inconsistencies or hallucinated content when compared to the source document. Performance is measured separately on hallucinated and factual summaries. We report both arithmetic mean accuracy (Acc-A), which averages the two scores but can be skewed by outliers, and harmonic mean accuracy (Acc-H), which offers a more balanced view by penalizing imbalanced performance. The dataset is available at: <https://github.com/RUCAIBox/HaluEval>.

Memory-intensive Datasets. To evaluate models on tasks that rely heavily on surface-level pattern matching rather than deep reasoning, we adopt a suite of memory-intensive benchmarks following [14]. These cover three categories: sentiment classification, textual entailment, and topic classification. For sentiment classification, we use SST-2 [49], MR [41], CR [21], RT [42], and HYP [28]. Textual entailment tasks include CB [8] and RTE [7], which require identifying whether a premise entails, contradicts, or is neutral to a hypothesis. For topic classification, we evaluate on AG News (AGN) [58] and Yahoo [59], which involve predicting the main topic of a given text. All tasks are evaluated using the same setup of [14]. These datasets are available at: <https://github.com/GSYfate/knnlm-limits/tree/main/data>.

C Implementation Details.

Training setting. We conduct our experiments on an $8 \times A800$ 80GB GPU setup. For language modeling, we use GPT2-xl to construct the key-value datastore and k NN-based distributions for training. We train MLP memory variants (small, medium, large) for 20,000 steps with learning rates of $2e-3$, $1e-3$, and $5e-4$ respectively, using a linear learning rate scheduler and the AdamW optimizer. For downstream tasks, including hallucination reduction, memory-intensive tasks, and reasoning, we use the Web-based datastore from [14] and evaluate across multiple backbone models: Llama-2-7B, Llama-3-8B, and Mistral-7B-v0.3. Each model is paired with a corresponding MLP memory module: 1.2B parameters for Llama-2-7B, 1.6B for Llama-3-8B, and 1.5B for Mistral-7B-v0.3. During training, we set the KL loss weight α to 0.4 and feed the MLP memory with hidden states from the transformer block at approximately 70% depth of the base model. The interpolation hyperparameter λ for language modeling is set to 0.25, while for downstream tasks, we follow the interpolation settings used in [14].

Test setting. For language modeling experiments, we utilize sliding window perplexity as the evaluation metric. Following k NN-LM [27], each test example uses a context length of 1024 tokens, with only the latter 512 tokens being scored. For evaluation on downstream tasks, we adopt the methodology from [14] and report results using the Domain Conditional Pointwise Mutual Information (DCPMI) scoring rule.

D Comparing Output Distribution Characteristics of LM, k NN, and MLP Memory

As two samples illustrated in Figure 4, distributions produced by LM, k NN search, and MLP memory exhibit distinct characteristics. LM typically yields smooth and dense probability distributions, as it is trained to generalize across large corpora and capture broad contextual patterns.

In contrast, the k NN approach produces sparse and spiky distributions, concentrating most of the probability mass on only a few retrieved neighbors. For instance, when using a GPT-2 model (vocabulary size 50,257), even after retrieving the top- k neighbors (e.g., $k = 1024$), only a small subset of these neighbors meaningfully influences the output distribution, while the majority receive near-zero probability.

The MLP memory lies between LMs and k NN in terms of distribution characteristics. As a neural model, it is trained using a combination of KL loss and CE loss to approximate the sparse and spiky distributions produced by the k NN approach. While its outputs remain somewhat smoother due to

the training objective, the resulting distributions are sharper than those of standard LMs, yet not as extreme as the highly concentrated outputs of k NN.

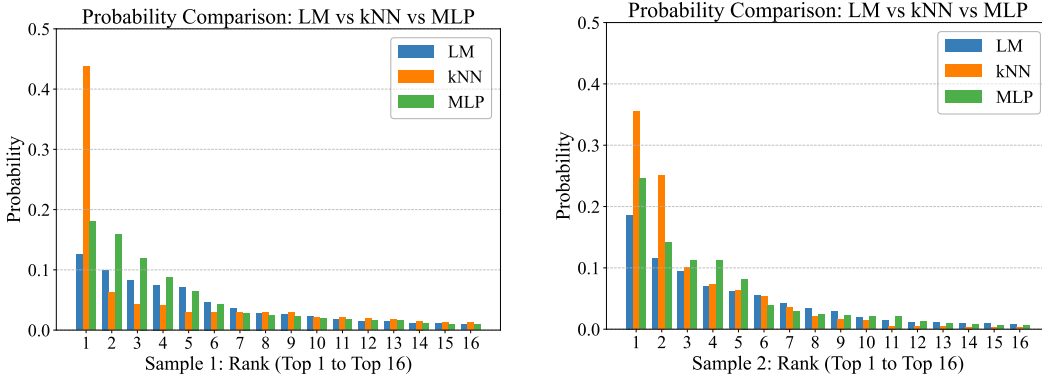


Figure 4: Comparison of output probability distributions. Two samples show the top-16 probabilities from the LM and k NN distributions using GPT2-large, along with the distribution generated by the MLP memory based on the same large model size.

Table 5 compares the output sparsity of LM, k NN, and MLP memory by reporting the number of tokens assigned non-zero probabilities at various thresholds. The LM assigns non-zero mass to all 50,257 tokens, reflecting its dense distribution. However, this number drops sharply at higher thresholds, with only 2 tokens receiving probabilities above 0.1, indicating a rapid decay despite its broad support.

In contrast, the k NN output is highly sparse, with only 251 tokens assigned any non-zero probability. Even at low thresholds (e.g., 10^{-6}), the number remains limited, confirming its concentrated nature shaped by a small set of retrieved neighbors.

MLP memory exhibits intermediate behavior. Although it outputs over the full vocabulary like the LM, the number of tokens exceeding higher thresholds aligns more closely with k NN. This suggests that MLP memory learns to approximate the spiky distributions of k NN while maintaining some smoothness from its parametric formulation.

Table 5: Number of tokens with non-zero probability mass at different thresholds. This table reports the number of tokens assigned non-zero probabilities by the LM, k NN, and MLP memory, across a range of probability thresholds. All values are averaged over 20,000 test samples.

Types	> 0.0	$> 10^{-6}$	$> 10^{-5}$	$> 10^{-4}$	$> 10^{-3}$	$> 10^{-2}$	$> 10^{-1}$
LM	50257	1760	562	148	34	7	2
k NN	251	217	197	146	43	9	2
MLP	50257	1151	388	115	30	7	2

Table 6 further examines distribution sharpness by reporting the number of top-ranked tokens needed to accumulate a specified proportion of total probability mass. Here, we observe that the k NN distribution reaches 99% cumulative probability with only 126 tokens, while the language model (LM) requires 617 tokens to achieve the same threshold. This suggests that the LM’s probability mass is more broadly spread across the vocabulary, in contrast to the highly concentrated outputs of k NN.

Interestingly, the MLP memory achieves 99% cumulative probability with 308 tokens, placing it between LM and k NN. Notably, the MLP reaches 80% total probability with only 13 tokens—fewer than both LM and k NN—indicating that it captures prominent signals more efficiently. These results support the observation that MLP memory produces sharper distributions than LMs, yet avoids the extreme sparsity of k NN.

Table 6: Cumulative token count required to reach probability mass thresholds. This table indicates the number of top-ranked tokens needed to accumulate a total probability mass exceeding thresholds such as 0.8, 0.9, etc. All values are averaged over 20,000 test samples.

Types	Top Prob Count(sum > 0.8)	sum > 0.9	sum > 0.95	sum > 0.99
LM	23	63	142	617
k NN	22	43	68	126
MLP	13	33	72	308

E Effect of Different k NN Target Distributions

Figure 5 presents the test perplexity of our overall model architecture evaluated at various training steps. In all settings, both the base language model and the MLP memory are of small size (GPT2-small), with the MLP memory trained to mimic k NN target distributions constructed from different base models: GPT2-small, GPT2-medium, GPT2-large, and GPT2-xl. As training progresses, test perplexity steadily declines across all variants, indicating stable optimization and effective learning. Among them, the model trained on the k NN-XL distribution achieves the lowest final test perplexity (12.84), closely followed by the one trained on k NN-large (12.85). In contrast, the models trained on k NN-medium and k NN-small converge to higher perplexities of approximately 12.87 and 12.91, respectively.

These results demonstrate that k NN target distributions derived from larger base models lead to improved performance when used to train the MLP memory. The richer and more informative supervision encoded in these distributions appears to enhance the parametric memory’s generalization ability.

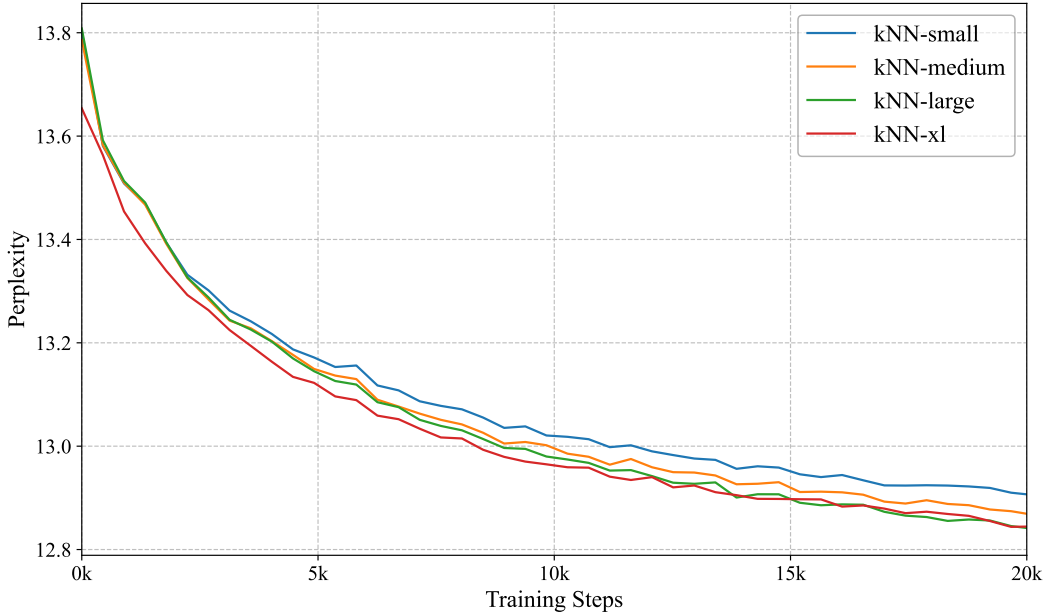


Figure 5: Test perplexity of our overall model architecture, where both the base language model and the MLP memory are of small size (GPT2-small). The MLP memory is trained to mimic different k NN target distributions constructed from various base models: k NN-small (GPT2-small), k NN-med (GPT2-medium), k NN-large (GPT2-large), and k NN-XL (GPT2-xl).

F Sensitivity to k in Target Distribution Generation

We used $k = 1024$ for generating all target distributions. Table 7 shows the sensitivity analysis using GPT2-large on WikiText-103. While smaller k values degrade performance, values beyond 1024 yield minimal gains while significantly increasing computational costs, making $k = 1024$ optimal for practical deployment.

Table 7: Test perplexity sensitivity to different values of k in target distribution generation using GPT2-large on WikiText-103.

Models	k	Perplexity
GPT2-large	—	10.43
+ k NN-LM	1	10.30
	2	10.11
	4	9.95
	8	9.83
	16	9.71
	32	9.63
	64	9.57
	128	9.52
	256	9.48
	512	9.46
	1024	9.43
	2048	9.42

G Sensitivity to Interpolation Weight λ

We evaluated the sensitivity of our method to the interpolation weight λ on TruthfulQA using Llama2-7B. Following established practice from k NN-LM, we use λ in the 0.2-0.3 range. Table 8 shows that our method achieves stable performance across different λ values, with optimal results at $\lambda = 0.3$. The consistent improvements across this range confirm that our gains are not due to hyperparameter overfitting.

Table 8: Performance sensitivity to different interpolation weights λ on TruthfulQA using Llama2-7B. We report means across 5 random seeds. Bold indicates best performance.

Models	TruthfulQA			AVG
	MC1	MC2	MC3	
Llama2-7B	26.58	41.88	18.94	29.13
+MLP Mem ($\lambda = 0.10$)	26.08	42.61	18.97	29.22
+MLP Mem ($\lambda = 0.15$)	26.08	42.97	19.22	29.42
+MLP Mem ($\lambda = 0.20$)	26.12	43.31	19.57	29.67
+MLP Mem ($\lambda = 0.25$)	26.12	43.65	19.63	29.80
+MLP Mem ($\lambda = 0.30$)	26.08	43.96	20.15	30.06
+MLP Mem ($\lambda = 0.40$)	25.44	44.53	20.01	29.99
+MLP Mem ($\lambda = 0.50$)	24.56	45.02	19.92	29.83